Perovskites

International Edition: DOI: 10.1002/anie.201702825
German Edition: DOI: 10.1002/ange.201702825

Low-Dimensional Organic Tin Bromide Perovskites and Their Photoinduced Structural Transformation

*Chenkun Zhou, Yu Tian, Mingchao Wang, Alyssa Rose, Tiglet Besara, Nicholas K. Doyle, Zhao Yuan, Jamie C. Wang, Ronald Clark, Yanyan Hu, Theo Siegrist, Shangchao Lin, and Biwu Ma**

Abstract: *Hybrid organic–inorganic metal halide perovskites possess exceptional structural tunability, with three- (3D), two- (2D), one- (1D), and zero-dimensional (0D) structures on the molecular level all possible. While remarkable progress has been realized in perovskite research in recent years, the focus has been mainly on 3D and 2D structures, with 1D and 0D structures significantly underexplored. The synthesis and characterization of a series of low-dimensional organic tin bromide perovskites with 1D and 0D structures is reported. Using the same organic and inorganic components, but at different ratios and reaction conditions, both 1D $(C_4N_2H_{14})SnBr_4$ and 0D $(C_4N_2H_{14}Br)_4SnBr_6$ can be prepared in high yields. Moreover, photoinduced structural transformation from 1D to 0D was investigated experimentally and theoretically in which photodissociation of 1D metal halide chains followed by structural reorganization leads to the formation of a more thermodynamically stable 0D structure.*

Hybrid organic–inorganic metal halide perovskites have received extraordinary research attention in recent years for their potential applications in various optoelectronic devices, ranging from photovoltaic cells (PVs) to light emitting diodes (LEDs) and optically pumped lasers.[1] As far as their compositions and structures are concerned, metal halide perovskites can be assembled using a variety of organic and inorganic components, with the basic building blocks (metal halide octahedrons, BX_6, where B is a metal and X is a halogen) arranged in different ways to exhibit 3D, 2D, 1D, and 0D structures.[2] In the 3D structure, small size cations, such as Cs^+ and $CH_3NH_3^+$, fit into the network formed by the corner-sharing metal halide octahedrons to form ABX_3. 2D perovskites have the BX_6 octahedrons connected in layered or corrugated sheets that are sandwiched between large organic cations, 1D perovskites have the BX_6 octahedrons connected in a chain (sharing corners, edges, or faces) and surrounded by organic cations, and 0D perovskites have the BX_6 octahedrons completely isolated from each other and surrounded by organic cations. Therefore, 2D, 1D, and 0D perovskites can be considered as the crystalline bulk assemblies of 2D, 1D, and 0D quantum confined materials, respectively. It should be pointed out that the 2D, 1D, and 0D perovskites on molecular level defined here are different from the morphological 2D nanosheets and nanoplatelets, 1D nanowires, and 0D nanoparticles based on 3D ABX_3.[3] While a significant amount of efforts has been dedicated to 3D and 2D perovskites with remarkable success, low-dimensional metal halide perovskites are still underexplored to date.

Recently, we reported the design, synthesis, and characterization of 1D organic lead bromide perovskites ($(C_4N_2H_{14}PbBr_4)$) and 0D tin bromide perovskites ($((C_4N_2H_{14}Br)_4SnBr_6)$).[4] In these 1D and 0D perovskites, the metal halide chains and molecules are surrounded by the same organic cations to form bulk assemblies of 1D and 0D core–shell quantum confined materials. These low-dimensional metal halide perovskites exhibit unique photophysical properties owing to strong quantum confinement. Unlike conventional 3D and 2D perovskites exhibiting narrow emissions with small Stokes shifts owing to delocalized excitonic character, these 1D and 0D perovskites have broadband emissions with large Stokes shifts as a result of localized exciton self-trapping in the quantum confined 1D and 0D structures. Despite these demonstrations of these 1D and 0D structures using the same organic cations, the design principles to obtain low-dimensional metal halide perovskites with controlled structures and compositions in a rational manner have not yet been established.

Herein we report synthetic control of low-dimensional tin bromide perovskites. By carefully controlling the reaction conditions, either 1D or 0D tin bromide perovskites can be prepared in high yield and excellent reproducibility. More interestingly, photoinduced structural transformation from 1D to 0D tin bromide perovskites was observed and characterized experimentally and theoretically for the first time. This finding, together with previously reported similar structural transformation from 3D $CH_3NH_3PbI_3$ to 0D $(CH_3NH_3)_4PbI_6{\cdot}2H_2O$,[5] suggests that the metal halide bond breaking can happen upon photoexcitation followed by structural reorganization, and individual metal halide octa-

[*] C. Zhou, N. K. Doyle, Dr. Z. Yuan, Prof. T. Siegrist, Prof. B. Ma
Department of Chemical and Biomedical Engineering
FAMU-FSU College of Engineering (USA)
E-mail: bma@fsu.edu
Y. Tian, M. Wang, Prof. Y. Hu, Prof. T. Siegrist, Prof. S. Lin, Prof. B. Ma
Materials Science and Engineering Program
Florida State University (USA)
A. Rose, J. C. Wang, Prof. R. Clark, Prof. Y. Hu, Prof. B. Ma
Department of Chemistry and Biochemistry, Florida State University (USA)
M. Wang, Prof. S. Lin
Department of Mechanical Engineering
FAMU-FSU College of Engineering (USA)
T. Besara, Prof. T. Siegrist
National High Magnetic Field Laboratory
Florida State University (USA)

Supporting information for this article can be found under: https://doi.org/10.1002/anie.201702825.

hedrons could be more thermodynamically stable than connected ones.

1D and 0D Sn bromide perovskite crystals were prepared by carefully controlling the reactant ratios of Sn^{II} bromide ($SnBr_2$) and *N,N′*-dimethylethylenediaminium bromide ($C_4N_2H_{14}Br_2$), as well as the synthetic conditions (Scheme 1). 1D Sn bromide perovskite crystals

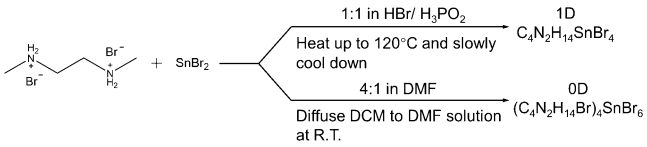

Scheme 1. The synthesis of the 1D and 0D Sn bromide perovskites.

($C_4N_2H_{14}SnBr_4$) were synthesized by reacting equal amounts of $SnBr_2$ and $C_4H_{14}N_2Br_2$ in a mixture of 48% w/w aqueous hydrobromic acid (HBr) and 50% w/w aqueous hypophosphorous acid (H_3PO_2) solution. H_3PO_2 was used to prevent the oxidation of Sn^{II}. The acid solution was heated up to 120 °C under stirring to dissolve the bromide salts completely. The crystals were grown after the stir was stopped and the temperature was slowly decreased to room temperature. To obtain high-quality and large needle-shaped crystals, the precursor solution was prepared in low concentration to slow down the crystal growth process, leading to a yield of about 15%. A higher chemical yield of about 60% was obtained by increasing the solution concentration, which however resulted in small needle-shaped crystals. Interestingly, the products prepared by this hydrothermal approach were dominated by 1D perovskites regardless of the reagent ratio of $C_4H_{14}N_2Br_2$ to $SnBr_2$ even at 4/1. Therefore, it is reasonable to assume that 1D perovskites could be kinetically favored products forming quickly during the fast hydrothermal crystal growth process. 0D $(C_4N_2H_{14}Br)_4SnBr_6$ crystals were prepared following the previously reported procedure, by diffusing dichloromethane (DCM) into a clear precursor solution of $C_4H_{14}N_2Br_2$ and $SnBr_2$ with the ratio of 4/1 in a nitrogen-filled glove box.

The crystal structures of low-dimensional Sn bromide perovskites were determined using single-crystal X-ray diffraction (SCXRD), as shown in Figure 1. 1D $C_4N_2H_{14}SnBr_4$ shows a similar crystal structure as $C_4N_2H_{14}PbBr_4$ in which the metal halide chains $[SnBr_4^{2-}]_\infty$ are surrounded by $C_4N_2H_{14}^{2+}$ cations to form bulk assembly of core–shell quantum wires. The average Sn–Br bond distance (3.022 Å) in $C_4N_2H_{14}SnBr_4$ is slightly shorter than that of Pb–Br (3.032 Å) in $C_4N_2H_{14}PbBr_4$. Considering the smaller covalent radius of Sn atom (ca. 1.39 Å) than that of Pb atom (ca. 1.46 Å), the relatively long Sn–Br bond indicates a much less efficient packing with weaker interactions between Sn and Br atoms, which could lead to an easier structural distortion in the excited states. The crystal structure of 0D $(C_4N_2H_{14}Br)_4SnBr_6$ has been reported before.[4b]

The photophysical properties of these low-dimensional Sn bromide perovskites were fully characterized using UV/Vis absorption spectrometry, as well as steady-state and time-resolved photoluminescence spectroscopy. Figure 2a shows the as-prepared 1D and 0D Sn bromide perovskite crystals

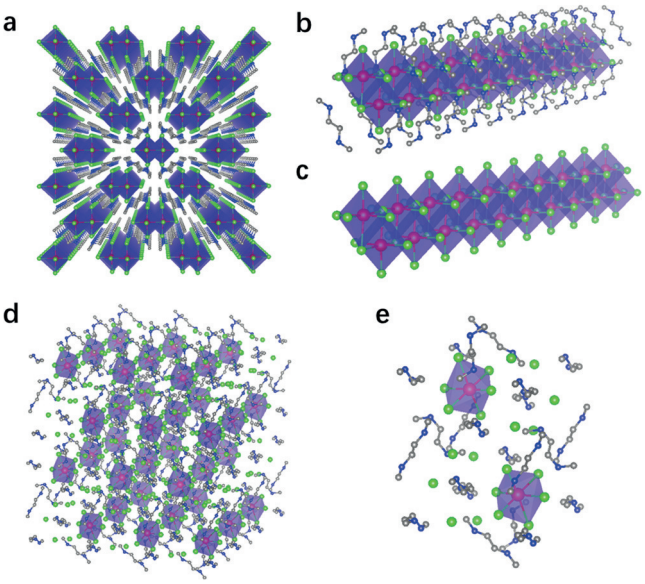

Figure 1. Crystal structures of 1D and 0D tin bromide perovskite crystals. a) Crystal structure of 1D Sn bromide perovskite $C_4N_2H_{14}SnBr_4$ (Sn red, Br green, N blue, C gray; hydrogen atoms were hidden for clarity). b) Views of a 1D Sn bromide wire wrapped by organic cations. c) Views of an individual 1D Sn bromide wire with edge sharing octahedrons. d) Crystal structure of 0D Sn bromide perovskite $(C_4N_2H_{14}Br)_4SnBr_6$. e) Crystal structure of 0D Sn bromide perovskite unit cell.

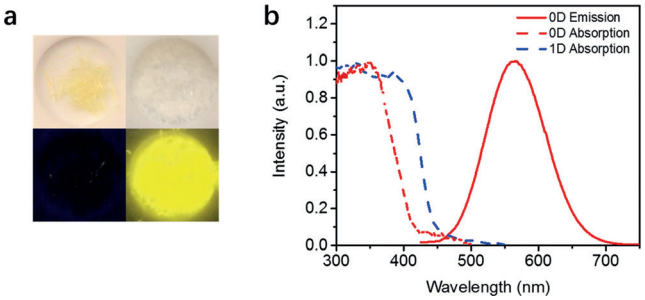

Figure 2. Photophysical properties of 1D and 0D Sn bromide perovskites. a) Images of 1D $C_4N_2H_{14}SnBr_6$ and 0D $(C_4N_2H_{14}Br)_4SnBr_6$ under ambient light and UV irradiation. b) Absorption spectra of 1D $C_4N_2H_{14}SnBr_6$ and 0D $(C_4N_2H_{14}Br)_4SnBr_6$, as well as emission spectrum of 0D $(C_4N_2H_{14}Br)_4SnBr_6$.

under ambient light and UV irradiation. The 1D $C_4N_2H_{14}SnBr_6$ crystals have a yellowish needle shape with no emission observed, while 0D $(C_4N_2H_{14}Br)_4SnBr_6$ crystals are colorless chunks exhibiting highly luminescent yellow emission. From the UV/Vis spectra shown in Figure 2b, 1D $C_4N_2H_{14}SnBr_6$ has a band edge at around 400 nm, which is clearly red-shifted compared to that of 0D $(C_4N_2H_{14}Br)_4SnBr_6$ at around 360 nm. This shift is not surprising if we consider that 1D structure has a weaker quantum confinement with a lower energy gap than 0D structure. Unlike strong bluish white-light emission observed in 1D lead bromide perovskites ($C_4N_2H_{14}PbBr_6$), no emission was detected from 1D $C_4N_2H_{14}SnBr_6$. This non-emissive property suggests new non-radiative decay processes present in 1D Sn bromide

perovskites that are not pronounced in 1D $C_4N_2H_{14}PbBr_6$. Considering the much smaller size of Sn compared to Pb, 1D $C_4N_2H_{14}SnBr_6$ has a much less efficiently packed and thus more flexible structure than $C_4N_2H_{14}PbBr_6$. Therefore, 1D $C_4N_2H_{14}SnBr_6$ is more susceptible to structural distortion in the excited state than 1D $C_4N_2H_{14}PbBr_6$, which can serve as non-radiative channels.

Interestingly, the non-emissive 1D Sn bromide perovskites became emissive (yellow light) upon continuous UV irradiation and the emission intensity enhanced as the exposure time increased, as shown in Figure 3a,b. The

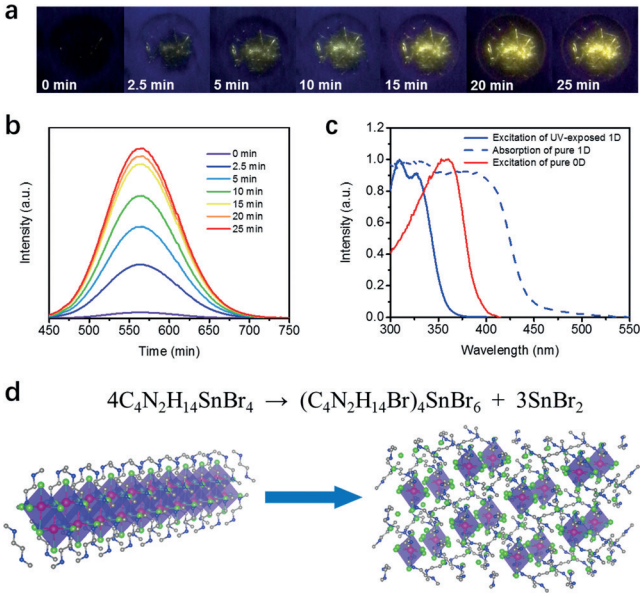

Figure 3. Photophysical properties of emissive species generated on the surface of 1D perovskites upon UV irradiation. a) Photographs of 1D Sn bromide perovskite crystals under UV irradiation. b) Luminescence intensities of 1D Sn bromide perovskite crystals under UV irradiation; c) the excitation spectra of emissive species generated by UV irradiation; d) proposed reaction for the photoinduced structural transformation.

excitation spectrum of this yellow emission in Figure 3c does not match the absorption spectrum of 1D $C_4N_2H_{14}SnBr_6$, suggesting the formation of a new emissive species upon UV exposure. As this emissive species exhibited exactly the same emission spectrum as that of highly stable 0D tin bromide perovskites ($(C_4N_2H_{14}Br)_4SnBr_6$), we hypothesized that there was a photoinduced structural transformation from 1D to 0D though a reaction shown in Figure 3d, in which the 1D perovskite is decomposed into 0D structure and $SnBr_2$. This non-radiative excited-state structural reorganization could well explain why 1D Sn bromide perovskites are not emissive at all. A similar photoinduced structural transformation from 3D methyl ammonium lead(II) iodide ($CH_3NH_3PbI_3$) to 0D $(CH_3NH_3)_4PbI_6{\cdot}2H_2O$ in present of water has been well-documented,[5] suggesting the possibility of photodissociation of metal halide bonds followed by structural reorganization in metal halide perovskites. Unlike 0D $(CH_3NH_3)_4PbI_6{\cdot}2H_2O$ with low stability that can further decompose to PbI_2, 0D $(C_4N_2H_{14}Br)_4SnBr_6$ has extremely high stability in the ambient condition. Considering the low surface-to-volume ratio of bulk crystals, the photoinduced structural transformation likely took place on the surface, resulting in bulk 1D perovskite crystals coated with emissive 0D perovskites. This is consistent with the blue-shifted excitation spectrum of the emissive species compared to that of pure 0D perovskites, as there is strong absorption from the core 1D perovskites.

To confirm the photoinduced structural transformation from 1D to 0D Sn bromide perovskites on the surface, structural characterizations using powder X-ray diffraction (PXRD) and solid-state NMR (SSNMR) were performed before and after UV exposure. To ensure detectable signals, 1D Sn bromide perovskite crystals were ground into powders in a small amount of acetone. A compact hand UV lamp (365 nm, 4 Watts) was then used to turn the non-emissive powders into highly luminescent ones by illuminating the powders for 30 min. PXRD were recorded for the UV exposed samples, as well as pure 1D and 0D Sn bromide perovskites, with the results shown in Figure 4a. In the PXRD pattern of UV exposed 1D Sn bromide perovskites, peaks from both 1D and 0D were clearly displayed, suggesting the formation of 0D perovskites in the 1D perovskite crystals. High-resolution solid-state ^{1}H NMR spectra of the 0D, 1D, and the UV exposed 1D perovskite crystals shown in Figure 4b exhibit significant difference. The ^{1}H spectrum of the 1D perovskites shows a sharp resonance at 7.4 ppm, which is assigned to NH_2^+. Furthermore, a broad resonance centered at 3.0 ppm with a full-width at half-maximum of 0.4 kHz is observed, which is from strongly coupled protons of CH_2 and CH_3 in the 1D peorvksite crystals. A weak resonance at about

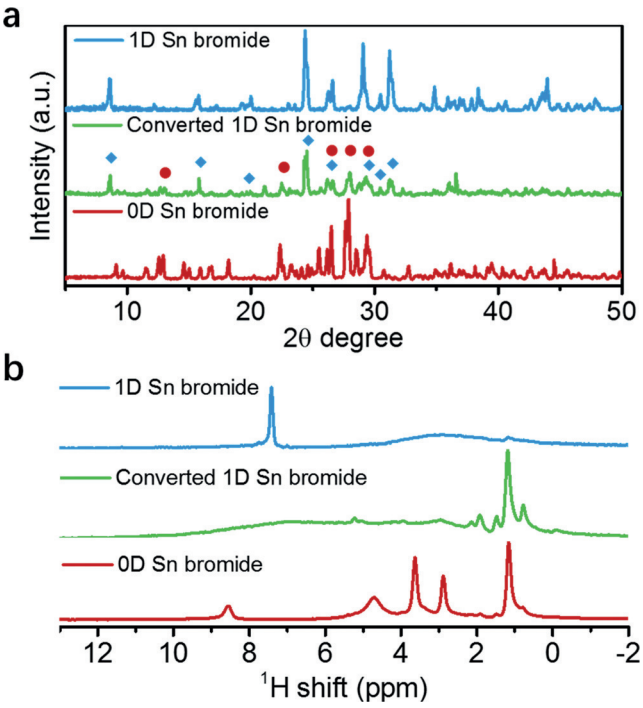

Figure 4. a) PXRD of tin bromide perovskite crystal powders. (blue ◆: patterns from 1D Sn bromide; red ●: patterns from 0D Sn bromide). b) Solid-state ^{1}H NMR spectra of Sn bromide perovskite crystals.

1 ppm is likely from protons on the $[SnBr_4^{2-}]_\infty$ surface. The surface of $[SnBr_4^{2-}]_\infty$ is largely covered by the organic moieties in the ordered 1D structure and the exposed surface area is expected to be small, and therefore the 1 ppm resonance is very weak. This 1 ppm resonance becomes more intense when the organic species gradually dissociate from the $[SnBr_4^{2-}]_\infty$ surface as the transition from the 1D structure to 0D structure occurs. Small satellite resonances around 1 ppm appear due to the heterogeneous local environments on the metal halide surfaces. In addition to a cluster of ^{1}H NMR peaks between 0 and 2 ppm from surface protons, an extremely broad peak spanning from 2 ppm to 10 ppm is shown in the ^{1}H NMR spectrum of the UV exposed 1D sample. The great breadth of this peak suggests that the organic species are still bound to the metal halide surfaces but very disordered. The lack of molecular mobility combined with structural disorder results in unresolved individual resonances. Once the organic molecules are completely reorganized, better resolution is achieved. Therefore, ^{1}H NMR of the 0D sample shows resolved resonances at 2.9 ppm from CH_3 protons and at 3.5 ppm from CH_2 protons. The ^{1}H resonance for NH_2^+ shifts to lower field with a large ppm value of 8.5, compared with that in the 1D sample, suggesting stronger deshielding and greater ionicity. The strong ^{1}H peak at about 1.0 ppm and the relatively broad one at 4.8 ppm are from surface protons and absorbed H_2O, respectively. These experimental results verified our hypothesis that partial dissociation of the 1D structure to form 0D structure occurs upon UV exposure.

Unlike unstable 0D $(CH_3NH_3)_4PbI_6{\cdot}2H_2O$ undergoing further decomposition to PbI_2, little-to-no transformation from 0D $(C_4N_2H_{14}Br)_4SnBr_6$ to $SnBr_2$ was observed in bulk Sn bromide perovskite crystals, which is consistent with the excellent photo- and thermostability of 0D perovskites in N_2 and ambient condition. The higher stability of 0D than 1D perovskites was further confirmed by theoretical calculations. We performed molecular dynamics (MD) simulations to study the structural and energetic properties of 0D $(C_4N_2H_{14})4SnBr_6$ and 1D $(C_4N_2H_{14})SnBr_4$ perovskites (see the Supporting Information for details of the simulation method). The MD-equilibrated crystal structures of 0D and 1D perovskites are very stable under the NVT ensemble at 300 K, confirming the capability of our developed force field to capture the structural properties of these low-dimensional metal halide perovskites. As proposed above, a balanced reaction from 1D to 0D perovskites follows: $4[(C_4N_2H_{14})SnBr_4] \rightarrow (C_4N_2H_{14}Br)_4SnBr_6 + 3[SnBr_2]$. MD simulations predicted a potential energy of -396.5 kcal mol^{-1} for 1D $(C_4N_2H_{14})SnBr_4$, -641 kcal mol^{-1} for 0D $(C_4N_2H_{14}Br)_4SnBr_6$, and -346.3 kcal mol^{-1} for $SnBr_2$. Therefore, 0D $(C_4N_2H_{14}Br)_4SnBr_6$ possesses a much lower energy than 1D $(C_4N_2H_{14})SnBr_4$, and the energy required for the above conversion reaction is -94 kcal mol^{-1}, suggesting that the above 1D to 0D perovskite conversion is thermodynamically spontaneous. The computational studies confirmed that 0D $(C_4N_2H_{14})_4SnBr_{10}$ is energetically more stable than 1D $(C_4N_2H_{14})SnBr_4$, consistent with our experimental observations.

In summary, we have demonstrated the synthetic control of low-dimensional organic tin bromide perovskites and found that the pathway to 1D $C_4N_2H_{14}SnBr_4$ is kinetically favored and the pathway to 0D $(C_4N_2H_{14}Br)_4SnBr_6$ is more thermodynamically favored. Photoinduced structural transformation from 1D to 0D involving photodissociation of metal halide bonds followed by structural reorganization has been observed and characterized by crystallographic analysis, spectroscopic methods, and molecular dynamics simulations. Our findings extend the capability of assemble organic–inorganic hybrid materials with controlled structures in a rational manner and help to gain a better understanding of the photostability issues of metal halide perovskites. Studying the excited-state structures of this new class of materials using time-resolved pump–probe X-ray diffraction and ultrafast spectroscopy will be attempted and reported in due course.

Acknowledgements

The authors acknowledge the Florida State University for financial support through the Energy and Materials Initiative. T.B. and T.S. acknowledge support by the National High Magnetic Field Laboratory, which is supported by the NSF cooperative agreement DMR-1157490 and the State of Florida. J.C.W. is supported by the National Science Foundation Graduate Research Fellowship under Grant No. DGE-1449440. The authors also thank Dr. Hanwei Gao for providing access to the instrument for photostability test.

Conflict of interest

The authors declare no conflict of interest.

Keywords: low-dimensional structures · metal halide perovskites · photoinduced structural change · photoluminescence · tin

How to cite: *Angew. Chem. Int. Ed.* **2017**, *56*, 9018–9022
Angew. Chem. **2017**, *129*, 9146–9150

[1] a) A. Kojima, K. Teshima, Y. Shirai, T. Miyasaka, *J. Am. Chem. Soc.* **2009**, *131*, 6050–6051; b) J. Burschka, N. Pellet, S. J. Moon, R. Humphry-Baker, P. Gao, M. K. Nazeeruddin, M. Gratzel, *Nature* **2013**, *499*, 316–319; c) X. Li, D. Q. Bi, C. Y. Yi, J. D. Decoppet, J. S. Luo, S. M. Zakeeruddin, A. Hagfeldt, M. Gratzel, *Science* **2016**, *353*, 58–62; d) Z. K. Tan, R. S. Moghaddam, M. L. Lai, P. Docampo, R. Higler, F. Deschler, M. Price, A. Sadhanala, L. M. Pazos, D. Credgington, F. Hanusch, T. Bein, H. J. Snaith, R. H. Friend, *Nat. Nanotechnol.* **2014**, *9*, 687–692; e) Y. C. Ling, Z. Yuan, Y. Tian, X. Wang, J. C. Wang, Y. Xin, K. Hanson, B. W. Ma, H. W. Gao, *Adv. Mater.* **2016**, *28*, 305–311; f) Y. Ling, Y. Tian, X. Wang, J. Wang, J. Knox, F. Perez-Orive, Y. Du, L. Tan, K. Hanson, B. Ma, H. Gao, *Adv. Mater.* **2016**, https://doi.org/10.1002/adma.201602513; g) G. C. Xing, N. Mathews, S. S. Lim, N. Yantara, X. F. Liu, D. Sabba, M. Gratzel, S. Mhaisalkar, T. C. Sum, *Nat. Mater.* **2014**, *13*, 476–480; h) H. M. Zhu, Y. P. Fu, F. Meng, X. X. Wu, Z. Z. Gong, Q. Ding, M. V. Gustafsson, M. T. Trinh, S. Jin, X. Y. Zhu, *Nat. Mater.* **2015**, *14*, 636–U115; i) S. W.

Eaton, M. L. Lai, N. A. Gibson, A. B. Wong, L. T. Dou, J. Ma, L. W. Wang, S. R. Leone, P. D. Yang, *Proc. Natl. Acad. Sci. USA* **2016**, *113*, 1993 – 1998.

[2] a) D. B. Mitzi, *J. Chem. Soc. Dalton Trans.* **2001**, 1 – 12; b) D. B. Mitzi, *J. Mater. Chem.* **2004**, *14*, 2355 – 2365; c) Z. Y. Cheng, J. Lin, *CrystEngComm* **2010**, *12*, 2646 – 2662; d) S. González-Carrero, R. E. Galian, J. Perez-Prieto, *Part. Part. Syst. Charact.* **2015**, *32*, 709 – 720; e) B. Saparov, D. B. Mitzi, *Chem. Rev.* **2016**, *116*, 4558 – 4596; f) Z. Yuan, Y. Shu, Y. Tian, Y. Xin, B. W. Ma, *Chem. Commun.* **2015**, *51*, 16385 – 16388; g) Z. Yuan, Y. Shu, Y. Xin, B. W. Ma, *Chem. Commun.* **2016**, *52*, 3887 – 3890.

[3] a) Q. A. Akkerman, S. G. Motti, A. R. S. Kandada, E. Mosconi, V. D'Innocenzo, G. Bertoni, S. Marras, B. A. Kamino, L. Miranda, F. De Angelis, A. Petrozza, M. Prato, L. Manna, *J. Am. Chem. Soc.* **2016**, *138*, 1010 – 1016; b) M. J. Ashley, M. N. O'Brien, K. R. Hedderick, J. A. Mason, M. B. Ross, C. A. Mirkin, *J. Am. Chem. Soc.* **2016**, *138*, 10096 – 10099; c) S. Bai, Z. C. Yuan, F. Gao, *J. Mater. Chem. C* **2016**, *4*, 3898 – 3904.

[4] a) Z. Yuan, C. K. Zhou, Y. Tian, Y. Shu, J. Messier, J. C. Wang, L. J. van de Burgt, K. Kountouriotis, Y. Xin, E. Holt, K. Schanze, R. Clark, T. Siegrist, B. W. Ma, *Nat. Commun.* **2017**, *8*, 14051; b) C. Zhou, Z. Yuan, Y. Tian, H. Lin, R. Clark, B. Chen, L. Burgt, J. Wang, K. Hanson, Q. Meisner, J. Neu, T. Besara, T. Siegrist, E. Lambers, P. Djurovich, B. Ma, *arXiv* **2017**, 1702.07200.

[5] a) J. S. Manser, M. I. Saidaminov, J. A. Christians, O. M. Bakr, P. V. Kamat, *Acc. Chem. Res.* **2016**, *49*, 330 – 338; b) A. M. A. Leguy, Y. Hu, M. Campoy-Quiles, M. I. Alonso, O. J. Weber, P. Azarhoosh, M. van Schilfgaarde, M. T. Weller, T. Bein, J. Nelson, P. Docampo, P. R. F. Barnes, *Chem. Mater.* **2015**, *27*, 3397 – 3407.

Manuscript received: March 17, 2017
Accepted manuscript online: June 1, 2017
Version of record online: July 3, 2017

